An $M : N$ Shared Regenerator Protection Scheme in Translucent WDM Networks

Elias A. Doumith
TICKET Lab - Antonine University
B.P. 40016 Hadat-Baabda - Lebanon
Email: elias.doumith@ua.edu.lb

Sawsan Al Zahr
LTCI - Telecom ParisTech - Université Paris-Saclay
46, rue Barrault F 75634 Paris Cedex 13 - France
Email: sawsan.alzahr@telecom-paristech.fr

***Abstract*—Most studies addressing translucent network design targeted a tradeoff between minimizing the number of deployed regenerators and minimizing the number of regeneration nodes. The latter highly depends on the carrier's strategy and is motivated by various considerations such as power consumption, maintenance and supervision costs. However, concentrating regenerators into a small number of nodes exposes the network to a high risk of data loss in the eventual case of regenerator pool failure. In this paper, we address the problem of survivable translucent network design taking into account the simultaneous effect of four transmission impairments. We propose an exact approach based on a mathematical formulation to solve the problem of regenerator placement while ensuring the network survivability in the hazardous event of a regenerator pool failure. For this purpose, for each accepted request requiring regeneration, we determine several routing paths along with associated valid wavelengths going through different regeneration nodes. In doing so, we implement an $M : N$ shared regenerator protection scheme. Simulation results highlight the gain obtained by reducing the number of regeneration nodes without sacrificing network survivability.**

I. Introduction

The demands for higher bandwidth at lower cost is increasing substantially in today's communication networks. End-users are using more applications that require reliable connectivity and faster data transfer. This constant growth of broadband services is pushing service providers and equipment vendors to look for scalable optical networks. However, the major limitations to scalability are the optical signal reach and the power consumption. Indeed, transmission impairments induced by long-haul optical equipment may significantly degrade the quality of the optical signal [1], [2]. In order to compensate for the signal degradation and to extend the signal reach, 3R (reamplification, reshaping, and retiming) regenerators may be deployed in the network which will increase the deployment cost as well as the power consumption. Thus, the only viable solution for most wide-area networks is the translucent approach where a small number of regenerators will be deployed in the network.

Since the early 2000s, many researches have addressed the optimal design of translucent optical networks. These studies highlighted that an intelligent deployment of the 3R regenerators allows a translucent optical network to perform similarly to a fully opaque network [3], [4]. The early studies in this field tried to minimize the number of regenerators based on the network topology (such as the number of neighbors or the average distance to neighbors). Indeed, in [4]–[7], a few number of nodes, with the highest number of pre-computed shortest paths traversing them, are selected as regeneration nodes. Afterward, regenerators are assigned to traffic requests based on a QoT evaluation method. In contrast with [4]–[6], additional regeneration nodes may be added during the routing and wavelength assignment process in order to maximize the number of satisfied requests while minimizing the number of regenerators and regeneration nodes [7]. However, these approaches are not realistic as the regenerator placement does not account for signal degradation. Other studies targeted the minimization of the number of regenerators in order to satisfy a given static traffic matrix [3], [8]–[11]. It was until 2011 that the problem of regenerator placement has been first investigated under dynamic but deterministic traffic model [12]. Under such a traffic pattern, one can take advantage from the dynamics of the traffic model so that deployed regenerators may be shared among multiple time-disjoint requests.

ISBN 978-3-903176-08-9

In the early 2000s, all studies that addressed the regenerator placement problem were based on empirical laws or heuristic approaches [3], [8]. It was until 2008 that Pan *et al.* proposed in [9] the first exact approach for regenerator placement. The aim was to minimize the number of regeneration nodes under static traffic requests with $1+1$ protection scheme. The QoT constraint was considered as a maximum optical reach. Later on, two exact approaches were proposed taking into account different linear and nonlinear impairments [10], [11]. In these studies, the problem of regenerator placement was formulated as a virtual topology design problem where the QoT constraint was considered as a minimum admissible Q-factor. In [10], the network topology is represented by an equivalent graph where two non-adjacent nodes, interconnected by a path with an admissible Q-factor, are connected by a crossover edge in the equivalent graph. In [11], a set of pre-computed paths is selected and regenerators are deployed along these paths. By routing a set of static traffic requests on the virtual topology, the aim of the proposed approaches is to minimize the number of regenerators or the number of regeneration nodes.

In our previous works [12], [13], we proposed an exact formulation for the problem of translucent network design in order to determine the optimal number of regenerators and regeneration nodes. Instead of considering permanent/semi-permanent traffic requests commonly used for network design purposes, we considered a more generic and realistic traffic model referred to as Scheduled Lightpath Demands (SLDs). Such a model allows us to easily represent the dynamism of the traffic without losing its deterministic aspect required in order to design the network. In [14], we extended our work to account for the traffic forecast uncertainty. More precisely, instead of designing a translucent network that can accommodate a single set of traffic requests, we considered in the design phase different sets of traffic requests that correspond to the traffic forecasts at different epochs in the future. The resulting optimal translucent optical network design can be used to accommodate any of the considered traffic forecasts.

In all the previous works, researchers tried to achieve the optimal translucent network design motivated by restrictions on capital and operational expenditures (CapEx/OpEx). Such a design consists in achieving a trade-off between minimizing the number of regenerators and minimizing the number of regeneration nodes. As the number of deployed regenerators has been reduced to a minimum, their utilization ratio is relatively high exposing the network to a high risk of data loss in the eventual case of regenerator pool failure. Indeed, if a regenerator pool fails, most of the traffic requests that were planned to be regenerated at this node cannot be regenerated at the other operational regenerator pools because of their high utilization ratio. Subsequently, the impacted traffic requests will suffer from excessive optical signal degradation and their data will be lost. In order to ensure high network availability, the network typically has redundant hardware that makes it available despite failures. The same analysis is applicable if we investigate the failure of multi-channel all-optical regenerators instead of electrical regenerators pool [15].

In this paper, we target to achieve the optimal translucent network design taking into account both operational and backup regenerators. For this purpose, for each accepted request requiring regeneration, we determine several routing paths along with associated valid wavelengths going through different regeneration nodes. In doing so, we implement an $M : N$ shared regenerator protection scheme minimizing the number of regenerators and regeneration nodes without sacrificing network survivability. In order to shorten the time needed to reach the optimal regenerator deployment solution, we tighten the formulation by adding constraints that will help discard equivalent solutions without omitting the optimal solution. As for the QoT constraint, we consider a minimum admissible Q-factor reflecting the simultaneous effect of four well known transmission impairments, namely chromatic dispersion, polarization mode dispersion, amplified spontaneous emission, and self phase modulation.

The remainder of this paper is organized as follows. In Section II, we present a description of the investigated scenarios. Our approach of survivable translucent network design is provided in Section III followed in Section IV by an analysis of the numerical results. Finally, we draw our conclusions in Section V.

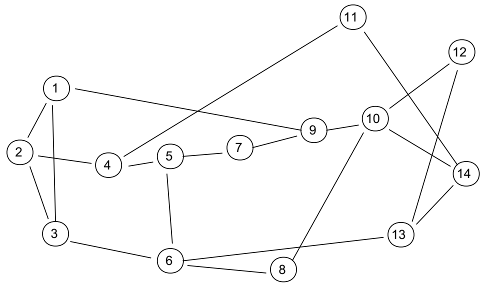

Links	Dist. (km)
u_1-u_2	480
u_1-u_3	680
u_1-u_9	1500
u_2-u_3	480
u_2-u_4	680
u_3-u_6	850
u_4-u_5	300
u_4-u_{11}	1500
u_5-u_6	480
u_5-u_7	400
u_6-u_8	850
u_6-u_{13}	1500
u_7-u_9	400
u_8-u_{10}	620
u_9-u_{10}	400
u_{10}-u_{12}	480
u_{13}-u_{14}	400
u_{10}-u_{14}	680
u_{11}-u_{14}	400
u_{12}-u_{13}	680

Fig. 1. The north American 14-node 20-link NSF backbone network.

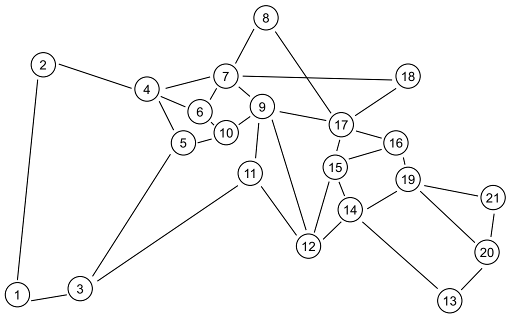

Links	Dist. (km)
u_1-u_2	1730
u_1-u_3	530
u_2-u_4	490
u_3-u_5	1110
u_3-u_{11}	1210
u_4-u_5	360
u_4-u_6	340
u_4-u_7	380
u_5-u_{10}	300
u_6-u_7	180
u_6-u_{10}	190
u_7-u_8	650
u_7-u_9	380
u_7-u_{18}	1150
u_8-u_{17}	670
u_9-u_{10}	210
u_9-u_{11}	400
u_{12}-u_{14}	540
u_{14}-u_{15}	280
u_{16}-u_{17}	310
u_{19}-u_{21}	680
u_{20}-u_{21}	310
u_9-u_{12}	1010
u_{12}-u_{15}	800
u_{14}-u_{19}	310
u_{16}-u_{19}	170
u_9-u_{17}	430
u_{13}-u_{14}	1140
u_{15}-u_{16}	60
u_{17}-u_{18}	540
u_{11}-u_{12}	730
u_{13}-u_{20}	550
u_{15}-u_{17}	260
u_{19}-u_{20}	660

Fig. 2. The European 21-node 34-link EBN backbone network.

II. Investigated Scenarios

A. Network Environment

A network node is modeled as an optical cross-connect (OXC) consisting of several wavelength selective switches (WSSs) and an access unit responsible for adding/dropping traffic requests [3], [16]. A limited number of network nodes are equipped with a pool of regenerators. A regenerator is a tunable transmitter-receiver pair along with a processing unit responsible for re-amplifying, re-shaping, and re-timing the optical signal in the electrical domain. A network link is composed of two unidirectional standard single mode fibers (one SMF in each direction) carrying each $W = 20$ wavelengths in the C-band. In order to compensate for the attenuation and the chromatic dispersion, double stage Erbium-doped fiber amplifiers (EDFAs) are deployed every 80 km along with dispersion compensating fibers (DCFs). Furthermore, inline optical gain equalizers are deployed every 400 km. For the numerical evaluation, we consider the 14-node 20-link NSF network (Figure 1) as well as the 21-node 34-link EBN network (Figure 2). Table I summarizes the parameters of all the equipment deployed in the network.

Transmission impairments induced by long-haul optical equipment accumulate along lightpaths and may significantly degrade the quality of the optical signal. We distinguish between two types of impairments, namely linear and non-

TABLE I
TRANSMISSION SYSTEM PARAMETERS

Parameter	Value
Number of wavelengths	20
Wavelengths (nm)	1538.97 – 1554.13
Channel spacing (GHz)	100
Channel bit rate (Gbps)	10
SMF input power (dBm)	−1
SMF loss (dB/km)	0.23

Parameter	Value
SMF PMD (ps/$\sqrt{km}$)	0.1
SMF dispersion (ps/nm.km)	$\stackrel{av.}{=} 17$[1]
DCF input power (dBm)	−7
DCF loss (dB/km)	0.6
DCF dispersion (ps/nm.km)	$\stackrel{av.}{=} -90$[1]
DCF PMD (ps/$\sqrt{km}$)	0.08

Parameter	Value
Switching loss (dB)	−13
Inline EDFA Noise Figure (dB)	$\stackrel{av.}{=} 6$[1]
Booster EDFA Noise Figure (dB)	$\stackrel{av.}{=} 5.25$[1]
Pre-compensation (ps)	−800
Dispersion slope $(ps/nm/span)$	100
Q-factor threshold (dB)	15.6

[1] It is only the mean value; the real value depends on the selected wavelength value.

linear impairments. Linear impairments are proportional to the traveled distance and depend on the signal itself (*e.g.,* chromatic dispersion CD, polarization mode dispersion PMD, amplified spontaneous emission ASE), while nonlinear impairments arise from the signal itself and from the interaction between neighboring channels (*e.g.,* self-phase modulation SPM, cross-phase modulation XPM, four wave mixing FWM) [17]. Various metrics can be used to evaluate the signal quality at the end of a lightpath. Among these metrics, the bit error rate (BER) is the most appropriate criterion because it aggregates the effects of all physical impairments. In this paper, we make use of "*BER-Predictor*" previously introduced in [18] to estimate the BER value at the end of each operational lightpath. BER-Predictor computes the Q-factor as a function of the penalties simultaneously induced by four physical impairments, namely ASE, CD, PMD, and SPM. The analytical relation between the Q-factor and the aforementioned impairments has been derived from analytical formulas and experimental measurements [2]. BER-Predictor can be used assuming either flat or non-flat spectral responses of optical equipment. A flat transmission system behaves the same regardless the wavelength value, while in a non-flat transmission system, the impairments induced by some equipment such as fibers and amplifiers depend on the wavelength value.

B. Traffic Model

In this paper, we make use of the SLD traffic model that allows us to capture the long-term aspect of the traffic as well as its dynamism. The i^{th} SLD request δ_i is represented by the tuple $(\mathfrak{s}_i, \mathfrak{r}_i, \alpha_i, \beta_i)$. The source node $\mathfrak{s}_i$ and the destination node $\mathfrak{r}_i$ of a request are chosen uniformly among the network nodes such that there is no demand between two adjacent nodes. The idea is to exclude one-hop lightpaths that do not require any regeneration. The attributes α_i and β_i denote the set-up and tear-down dates of a request. We first assume that all the requests arrive at the same time ($\alpha_i = 0, \ \forall i$) and, if accepted, will hold the network for the whole simulation period ($\beta_i = \Delta, \ \forall i$). Such requests are known as permanent lightpath demands (PLDs). Without changing the source and destination nodes of the requests, we then reduce the period where they are active according to a parameter π ($0 < \pi \leqslant 1$). More precisely, the activity period ($\beta_i - \alpha_i$) of a request δ_i is chosen uniformly in the interval $[\Delta \times \pi - 1, \Delta \times \pi + 1]$, and the set-up date α_i is chosen randomly while ensuring that δ_i still ends before the expiration of the simulation period ($\beta_i \leqslant \Delta$).

III. $M:N$ SHARED REGENERATOR PROTECTION SCHEME

We target to achieve the optimal translucent network design taking into account both operational and backup regenerators. These regenerators are required in order to cope with transmission impairments and for wavelength conversion needs. Given the network topology and the set of traffic requests, we seek to maximize the number of accepted requests. For each accepted request requiring regeneration, we determine several routing paths along with associated valid wavelengths going through different regeneration nodes. In doing so, we implement an $M:N$ shared regenerator protection scheme minimizing the number of regenerators and regeneration nodes without sacrificing network survivability. The optimal translucent network design is achieved by formulating the problem as a Mixed-Integer Linear Program and solving it using traditional solvers.

In order to improve the scalability of our approach, we decompose the problem into the "Routing and Regenerator Placement" (RRP) sub-problem and the "Wavelength Assignment and Regenerator Placement" (WARP) sub-problem. In the former, we place regenerators and route the traffic requests while assuming that the QoT is independent of the wavelength value. In the latter, additional regenerators may be required to overcome the dependency of the QoT on the wavelength value. Deployed regenerators may be shared among multiple non-concurrent requests. The common parameters for these two sub-problems are:

- The network topology represented by a graph $\mathcal{G} = (\mathcal{V}, \mathcal{E})$, where $\mathcal{V} = \{\mathfrak{u}_v, v = 1 \cdots N\}$ is the set of network nodes and $\mathcal{E} = \{\mathfrak{e}_e = (\mathfrak{u}_v, \mathfrak{u}_u) \in \mathcal{V} \times \mathcal{V}, e = 1 \cdots L\}$ is the set of unidirectional fiber-links connecting these nodes.
- The set of available wavelengths $\Lambda = \{\lambda_\ell, \ell = 1 \cdots W\}$ on each fiber-link in the network.
- The threshold Q_{th} for an admissible Q-factor.

As we are concerned by the failure of a regenerator pool that can be located at any node of the network, we consider, for each of the sub-problems, $N+1$ different scenarios. Scenario '0' corresponds to the case where all the regenerator pools are fully operational, while scenario 's' ($s = 1 \cdots N$) corresponds to the case where the regenerator pool at node $\mathfrak{u}_s$ is down.

A. Routing and Regenerator Placement

In this sub-problem, we assume that the QoT is independent of the wavelength value. In other words, the QoT of a lightpath transmitted over a wavelength λ_ℓ is the same as if the lightpath was transmitted over the reference wavelength $\lambda_c = 1550$ nm. This is obtained by setting BER-predictor to operate under the flat spectral response configuration. The RRP sub-problem is formulated as follows:

1) Parameters:

• The set of traffic requests $\mathcal{D} = \{\delta_i, i = 1\cdots D\}$. Each request δ_i is represented by a tuple $(\mathfrak{s}_i \in \mathcal{V}, \mathfrak{r}_i \in \mathcal{V}, \alpha_i, \beta_i)$.

• The ordered set $\mathcal{T}$ grouping the set-up and tear-down dates of all the requests in $\mathcal{D}$.

$$\mathcal{T} = \bigcup_{\delta_i \in \mathcal{D}} \{\alpha_i, \beta_i\} = \{\tau_1, \cdots, \tau_{\mathfrak{T}}\} \tag{1}$$

such that $\tau_1 < \tau_2 < \cdots < \tau_{\mathfrak{T}}$ and $\mathfrak{T} = |\mathcal{T}|$

• The request matrix $\Theta = \{\theta_{i,t}, i = 1\cdots D, t = 1\cdots\mathfrak{T}\}$ representing the traffic requests over time. An element $\theta_{i,t}$ of this matrix is a binary value specifying the presence $(\theta_{i,t} = 1)$ or the absence $(\theta_{i,t} = 0)$ of request δ_i at time instant τ_t.

$$\theta_{i,t} = \begin{cases} 1 & \text{if } \alpha_i \leqslant \tau_t < \beta_i, \\ 0 & \text{otherwise.} \end{cases} \tag{2}$$

• For each request δ_i, we compute K-shortest paths in terms of real length (*cf.* Figures 1 and 2) connecting its source node $\mathfrak{s}_i$ to its destination node $\mathfrak{r}_i$. Let $\mathcal{P}_i = \{p_{i,j}, j = 1\cdots K\}$ be the set of available shortest paths for request δ_i. The j^{th}-shortest path $p_{i,j}$ of δ_i is the ordered set of unidirectional links $\{\mathfrak{e}_{e_1}, \mathfrak{e}_{e_2}, \cdots, \mathfrak{e}_{e_{|p_{i,j}|}}\}$ traversed in the source-destination direction $(\mathfrak{s}_i \mapsto \mathfrak{r}_i)$.

• For each link pair $(\mathfrak{e}_m, \mathfrak{e}_n)$ along a path $p_{i,j}$, we compute by means of BER-Predictor the Q-factor value $\mathfrak{Q}_{i,j}^{m,n}$ of the directed path-segment delimited by the *source* node of link $\mathfrak{e}_m$ and the *destination* node of link $\mathfrak{e}_n$ $(\mathfrak{e}_m \preccurlyeq \mathfrak{e}_n)$. As we assumed a flat spectral response, $\mathfrak{Q}_{i,j}^{m,n}$ is constant for all the wavelengths along this directed path-segment.

2) Variables:

• The binary acceptance variables $\mathfrak{a}_i$, $i = 1\cdots D$.
$\mathfrak{a}_i = 1$, if request δ_i is accepted. $\mathfrak{a}_i = 0$, otherwise.

• The binary variables $\mathfrak{p}_{s,i,j}$, $s = 0\cdots N$, $i = 1\cdots D$, $j = 1\cdots K$.
$\mathfrak{p}_{s,i,j} = 1$, if in scenario 's', request δ_i is routed over the j^{th}-shortest path between $\mathfrak{s}_i$ and $\mathfrak{r}_i$. $\mathfrak{p}_{s,i,j} = 0$, otherwise.

• The binary variables $\zeta_{s,i,j}^{m,n}$, $s = 0\cdots N$, $i = 1\cdots D$, $j = 1\cdots K$, $m = 1\cdots L$, $n = 1\cdots L$.
$\zeta_{s,i,j}^{m,n}$ is an intermediate variable used to insure that the Q-factor at the end of the directed path-segment delimited by the source node of link $\mathfrak{e}_m$ and the destination node of link $\mathfrak{e}_n$ along the j^{th}-shortest path $p_{i,j}$ used by the request δ_i in scenario 's' exceeds the predefined threshold.

• The binary variables $\mathfrak{d}_{s,i,u}$, $s = 0\cdots N$, $i = 1\cdots D$, $u = 1\cdots N$.
$\mathfrak{d}_{s,i,u} = 1$, if in scenario 's', request δ_i is regenerated at node $\mathfrak{u}_u$. $\mathfrak{d}_{s,i,u} = 0$, otherwise.

• The non-negative integer variables $\psi_{s,u,t}$, $s = 0\cdots N$, $u = 1\cdots N$, $t = 1\cdots\mathfrak{T}$.
$\psi_{s,u,t}$ is equal to the number of regenerators that are in use in scenario 's' at node $\mathfrak{u}_u$ and time instant τ_t.

• The binary variables ϕ_u, $u = 1\cdots N$.
$\phi_u = 1$, if node $\mathfrak{u}_u$ is selected as a regeneration node. $\phi_u = 0$, otherwise.

• The non-negative integer variables $\mathfrak{R}_u$, $u = 1\cdots N$.
$\mathfrak{R}_u$ denotes the number of regenerators deployed at node $\mathfrak{u}_u$.

3) Constraints:

• If request δ_i is accepted, it is routed over a single path among the available K-shortest paths between $\mathfrak{s}_i$ and $\mathfrak{r}_i$ in each of the considered scenarios. $\forall s = 0\cdots N$, $\forall i = 1\cdots D$,

$$\sum_{j=1\cdots K} \mathfrak{p}_{s,i,j} = \mathfrak{a}_i \tag{3}$$

• In each scenario 's', the number of requests routed over a single fiber-link $\mathfrak{e}_m$ must not exceed, at any time, the number of wavelengths on that fiber-link. $\forall s = 0\cdots N$, $\forall t = 1\cdots\mathfrak{T}$, $\forall m = 1\cdots L$,

$$\sum_{i=1\cdots D} \theta_{i,t} \times \sum_{j=1\cdots K \setminus \mathfrak{e}_m \in p_{i,j}} \mathfrak{p}_{s,i,j} \leqslant W \tag{4}$$

• In each scenario 's', the Q-factor at the end of the path-segment delimited by any two distinct nodes along the selected path of an accepted request must exceed the predefined threshold Q_{th}. Otherwise, regenerators must be deployed at some intermediate nodes along this path-segment. This can be expressed mathematically as follows: $\forall s = 0\cdots N$, $\forall i = 1\cdots D$, $\forall j = 1\cdots K$, $\forall \mathfrak{e}_n \in p_{i,j}$,

$$\sum_{\mathfrak{e}_m \in p_{i,j} \setminus \mathfrak{e}_m \preccurlyeq \mathfrak{e}_n} \zeta_{s,i,j}^{m,n} \times \mathfrak{Q}_{i,j}^{m,n} \geqslant \mathfrak{p}_{s,i,j} \times Q_{th} \tag{5a}$$

$$\sum_{\mathfrak{e}_m \in p_{i,j} \setminus \mathfrak{e}_m \preccurlyeq \mathfrak{e}_n} \zeta_{s,i,j}^{m,n} = \mathfrak{p}_{s,i,j} \tag{5b}$$

• By collecting all the previous constraints on the variables $\zeta_{s,i,j}^{m,n}$, we can determine, for each scenario 's', all the intermediate nodes $\mathfrak{u}_u$ where request δ_i should be regenerated (except at its source node $\mathfrak{s}_i$). $\forall s = 0\cdots N$, $\forall i = 1\cdots D$, $\forall j = 1\cdots K$, $\forall \mathfrak{e}_m = (\mathfrak{u}_u, \mathfrak{u}_v) \in p_{i,j}$, $\forall \mathfrak{e}_n \in p_{i,j}$ such that $\mathfrak{e}_m \preccurlyeq \mathfrak{e}_n$ and $\mathfrak{u}_u \neq \mathfrak{s}_i$,

$$\mathfrak{d}_{s,i,u} \geqslant \zeta_{s,i,j}^{m,n} \tag{6}$$

• In each scenario 's', the number of regenerators $\psi_{s,u,t}$ in use at node $\mathfrak{u}_u$ and time instant τ_t can then be computed as: $\forall s = 0\cdots N$, $\forall u = 1\cdots N$, $\forall t = 1\cdots\mathfrak{T}$,

$$\psi_{s,u,t} = \sum_{i=1\cdots D} \theta_{i,t} \times \mathfrak{d}_{s,i,u} \tag{7}$$

• The number of regenerators $\mathfrak{R}_u$ deployed at node $\mathfrak{u}_u$ is the maximum number of regenerators that are in use at any time for all the considered scenarios. $\forall s = 0\cdots N$, $\forall u = 1\cdots N$, $\forall t = 1\cdots\mathfrak{T}$,

$$\mathfrak{R}_u \geqslant \psi_{s,u,t} \tag{8}$$

• A node is considered as a regeneration node if it hosts at least a single regenerator. $\forall u = 1\cdots N$,

$$\phi_u \geqslant 10^{-3} \times \mathfrak{R}_u \tag{9}$$

• Finally, regenerator pool failure at node $\mathfrak{u}_s$ is simulated by setting to zero the number of regenerators that can be deployed at this node in its corresponding scenario. $\forall s = 1\cdots N$, $\forall t = 1\cdots\mathfrak{T}$,

$$\psi_{s,s,t} = 0 \tag{10}$$

4) Objective: The objective of the RRP sub-problem is to maximize the number of accepted requests while minimizing the number of regenerators and regeneration nodes. This objective is expressed as:

$$\max \quad \gamma_1 \times \sum_{i=1\cdots D} \mathfrak{a}_i - \gamma_2 \times \sum_{u=1\cdots N} \phi_u - \gamma_3 \times \sum_{u=1\cdots N} \mathfrak{R}_u \quad (11)$$

where γ_1, γ_2, and γ_3 are three non-negative real numbers used to stress the regenerators concentration into a limited number of regeneration nodes, the minimization of the required number of regenerators, the maximization of the number of accepted requests, or any combination of the previous objectives.

5) Performance Improvement: Although the previous formulation is correct, the feasible solution space is quite large. In order to shorten the time needed to solve the RRP sub-problem, we reduce the solution space while paying attention to not omit the optimal solution. This is achieved by cutting regions of the solution space that do not contain any improvement. Indeed, if we notice that when node $\mathfrak{u}_s$ is not selected as a regeneration node, the scenario 's' representing the failure of the regenerator pool at this node is obvious as it should not affect the accepted requests nor their associated paths. More precisely, the paths assigned to the requests in scenario 's' should be identical to the paths obtained in scenario '0'. This is obtained by replacing Equation (3) with the following:

- If request δ_i is accepted in scenario '0' (no regenerator pool failure), it is routed over a single path $p_{i,j}$ among the available K-shortest paths between $\mathfrak{s}_i$ and $\mathfrak{r}_i$. $\forall i = 1 \cdots D$,

$$\sum_{j=1\cdots K} \mathfrak{p}_{0,i,j} = \mathfrak{a}_i \quad (12)$$

- For each failure scenario 's', if node $\mathfrak{u}_s$ is a regeneration node ($\phi_s = 1$), we select a single path $p_{i,j}$ for each accepted request δ_i. Conversely, if node $\mathfrak{u}_s$ is not a regeneration node ($\phi_s = 0$), we set all the variables $\mathfrak{p}_{s,i,j}$ to zero. In this way, we do not assign any path to the accepted requests. Once we obtain the optimal solution, we route, in a post-processing step, each accepted request in scenario 's' on the same path as in scenario '0'. This is expressed mathematically as: $\forall s = 1 \cdots N$, $\forall i = 1 \cdots D$,

$$\sum_{j=1\cdots K} \mathfrak{p}_{s,i,j} = \mathfrak{a}_i \times \phi_s \quad (13)$$

The expression $\mathfrak{a}_i \times \phi_s$ is non-linear since it is the product of two binary variables. However, this product can be linearized by means of additional constraints. Thus, Equation (13) can be written in linear form as follows: $\forall s = 1 \cdots N$, $\forall i = 1 \cdots D$,

$$\sum_{j=1\cdots K} \mathfrak{p}_{s,i,j} \leq \mathfrak{a}_i \quad (14a)$$

$$\sum_{j=1\cdots K} \mathfrak{p}_{s,i,j} \leq \phi_s \quad (14b)$$

$$\sum_{j=1\cdots K} \mathfrak{p}_{s,i,j} \geq \mathfrak{a}_i + \phi_s - 1 \quad (14c)$$

B. Wavelength Assignment and Regenerator Placement

In the solution obtained at the end of the RRP sub-problem, some requests are accepted; others are rejected. Rejected requests are definitely dropped and removed from the problem. Let $\widehat{\mathcal{D}} = \{\widehat{\delta}_i, i = 1 \cdots \widehat{D}\}$ be the set of accepted requests. Each accepted request has been assigned a single path between its source and its destination nodes in the normal operational scenario ($s = 0$) as well as in each considered failure scenario ($s = 1 \cdots N$). This request may have been regenerated at some intermediate nodes along its path. Without altering its selected path, an accepted request requiring regeneration in a particular scenario is divided into path-segments whenever it passes through its regeneration node. As the routes and the regenerators assigned to a given request may vary from one scenario to another, its decomposition into sub-paths will also vary. Let $\widetilde{\mathcal{D}}_s = \{\widetilde{\delta}_{s,d}, d = 1 \cdots \widetilde{D}_s\}$ be the modified sets of accepted requests (one modified set of requests for each considered scenario $s = 0 \cdots N$) containing the accepted requests with an admissible QoT (no regeneration required) as well as the path-segments of the accepted requests requiring regeneration.

In the WARP sub-problem, we assign to each request $\widetilde{\delta}_{s,d}$ in a scenario 's' a single continuous wavelength between its source and its destination nodes. When this is not possible, additional regenerators are deployed to serve as wavelength converters. Moreover, all these requests have an acceptable QoT if they are transmitted over the reference wavelength $\lambda_c = 1550$ nm. If a request $\widetilde{\delta}_{s,d}$ is transmitted over another wavelength, its QoT may be degraded due to the non-flat spectral response of optical equipment. This problem can be resolved by deploying additional regenerators at some intermediate nodes along the path assigned to $\widetilde{\delta}_{s,d}$. However, it may happen that the required additional regenerator for a request $\widetilde{\delta}_{s,d}$ in scenario 's' needs to be deployed at node $\mathfrak{u}_s$. Recalling that scenario 's' corresponds to the case where the regenerator pool at node $\mathfrak{u}_s$ is down, no regenerators can be deployed at node $\mathfrak{u}_s$ and the corresponding request will be rejected. In order to optimize the network ressources' utilization, whenever a request $\widetilde{\delta}_{s,d}$ is rejected, we also reject the original request $\widehat{\delta}_i$ and all its path-segments from all the scenarios. Furthermore, we remove all the regenerators that were required by the original request $\widehat{\delta}_i$ in the RRP sub-problem. For this purpose, we define the function $\mathfrak{F}(.)$ that returns, for each request $\widetilde{\delta}_{s,d} \in \widetilde{\mathcal{D}}_s$, the index of the associated original request $\widehat{\delta}_i \in \widehat{\mathcal{D}}$.

$$\mathfrak{F}\left(\widetilde{\delta}_{s,d}\right) = i \quad (15)$$

Finally, we take advantage of the regenerators deployed in the RRP sub-problem when they are not in use. Hence, the WARP sub-problem is formulated as follows:

1) Parameters:

- The set of original requests $\widehat{\mathcal{D}} = \{\widehat{\delta}_i, i = 1 \cdots \widehat{D}\}$ that were accepted in the RRP sub-problem. Each accepted original request $\widehat{\delta}_i$ is represented by a tuple $(\mathfrak{s}_i \in \mathcal{V}, \mathfrak{r}_i \in \mathcal{V}, \alpha_i, \beta_i)$.
- For each considered scenario 's', an accepted original request $\widehat{\delta}_i$ is routed over a single path and may be regenerated at some intermediate nodes along this path. This is captured by the binary parameters $\widehat{\mathfrak{d}}_{s,i,u}$, $s = 0 \cdots N$, $i = 1 \cdots \widehat{D}$, $u = 1 \cdots N$. $\widehat{\mathfrak{d}}_{s,i,u} = 1$, if original request $\widehat{\delta}_i$ was regenerated in scenario 's' of the RRP sub-problem at node $\mathfrak{u}_u$. $\widehat{\mathfrak{d}}_{s,i,u} = 0$, otherwise.
- The modified sets of requests $\widetilde{\mathcal{D}}_s = \{\widetilde{\delta}_{s,d}, d = 1 \cdots \widetilde{D}_s\}$ ($s = 0 \cdots N$) obtained by dividing the original requests into path-segments at the nodes where they were regenerated.

Each request $\widetilde{\delta}_{s,d}$ is represented by a tuple $(\mathfrak{s}_{s,d} \in \mathcal{V}, \mathfrak{r}_{s,d} \in \mathcal{V}, \alpha_{s,d}, \beta_{s,d})$.

- At the end of the RRP sub-problem, each request $\widetilde{\delta}_{s,d}$ is routed over a single path $p_{s,d}$ represented as the ordered set of unidirectional links $\{\mathfrak{e}_{e_1}, \mathfrak{e}_{e_2}, \cdots, \mathfrak{e}_{e_{|p_{s,d}|}}\}$ traversed in the source-destination direction $(\mathfrak{s}_{s,d} \mapsto \mathfrak{r}_{s,d})$. For each wavelength $\lambda_\ell \in \Lambda$, we compute by means of BER-Predictor the Q-factor value $\mathfrak{Q}^\ell_{s,d}$ at the destination node $\mathfrak{r}_{s,d}$ of the selected path $p_{s,d}$. In this sub-problem, BER-predictor operates under the non-flat spectral response configuration.
- The ordered set $\mathcal{T} = \{\tau_t, t = 1\cdots\mathfrak{T}\}$ grouping the set-up and tear-down dates of all the requests in $\widehat{\mathcal{D}}$ (*cf.* Equation (1)).
- The request matrix $\widehat{\Theta} = \{\widehat{\theta}_{i,t}, i = 1\cdots\widehat{D}, t = 1\cdots\mathfrak{T}\}$ representing the original requests $\widehat{\delta}_i$ over time. An element $\widehat{\theta}_{i,t}$ of this matrix is a binary value specifying the presence $(\widehat{\theta}_{i,t} = 1)$ or the absence $(\widehat{\theta}_{i,t} = 0)$ of request $\widehat{\delta}_i$ at time instant τ_t.

$$\widehat{\theta}_{i,t} = \begin{cases} 1 & \text{if } \alpha_i \leqslant \tau_t < \beta_i, \\ 0 & \text{otherwise.} \end{cases} \tag{16}$$

- For each scenario 's' $(s = 0\cdots N)$, the new request matrix $\widetilde{\Theta}_s = \{\widetilde{\theta}_{s,d,t}, d = 1\cdots\widetilde{D}_s,\ t = 1\cdots\mathfrak{T}\}$ representing the requests $\widetilde{\delta}_{s,d}$ over time. An element $\widetilde{\theta}_{s,d,t}$ of this matrix is a binary value specifying the presence $(\widetilde{\theta}_{s,d,t} = 1)$ or the absence $(\widetilde{\theta}_{s,d,t} = 0)$ of request $\widetilde{\delta}_{s,d}$ at time instant τ_t.

$$\widetilde{\theta}_{s,d,t} = \begin{cases} 1 & \text{if } \alpha_{s,d} \leqslant \tau_t < \beta_{s,d}, \\ 0 & \text{otherwise.} \end{cases} \tag{17}$$

2) Variables:

- The binary acceptance variables $\mathfrak{a}_i$, $i = 1\cdots\widehat{D}$.

$\mathfrak{a}_i = 1$, if original request $\widehat{\delta}_i$ is still accepted. $\mathfrak{a}_i = 0$, otherwise.

- The binary variables $\rho^\ell_{s,d,m}$, $s = 0\cdots N$, $d = 1\cdots\widetilde{D}_s$, $m = 1\cdots L$, $\ell = 1\cdots W$.

$\rho^\ell_{s,d,m} = 1$, if in scenario 's', request $\widetilde{\delta}_{s,d}$ is transmitted over wavelength λ_ℓ along link $\mathfrak{e}_m$. $\rho^\ell_{s,d,m} = 0$, otherwise.

- The binary variables $\mathfrak{d}_{s,d,u}$, $s = 0\cdots N$, $d = 1\cdots\widetilde{D}_s$, $u = 1\cdots N$.

$\mathfrak{d}_{s,d,u} = 1$, if in scenario 's', request $\widetilde{\delta}_{s,d}$ is regenerated in the WARP sub-problem at node $\mathfrak{u}_u$. $\mathfrak{d}_{s,d,u} = 0$, otherwise.

- The non-negative integer variables $\psi_{s,u,t}$, $s = 0\cdots N$, $u = 1\cdots N$, $t = 1\cdots\mathfrak{T}$.

$\psi_{s,u,t}$ is equal to the number of regenerators that are in use in scenario 's' at node $\mathfrak{u}_u$ and time instant τ_t.

- The binary variables ϕ_u, $u = 1\cdots N$.

$\phi_u = 1$, if node $\mathfrak{u}_u$ is a regeneration node. $\phi_u = 0$, otherwise.

- The non-negative integer variables $\mathfrak{R}_u$, $u = 1\cdots N$.

$\mathfrak{R}_u$ denotes the total number of regenerators deployed at node $\mathfrak{u}_u$ (including those already deployed in the RRP sub-problem).

3) Constraints:

- If original request $\widehat{\delta}_i$ remains accepted, a single wavelength is reserved on all the links that are traversed by its sub-paths $\widetilde{\delta}_{s,d}$ in all the scenarios. $\forall s = 0\cdots N, \forall d = 1\cdots\widetilde{D}_s, \forall m = 1\cdots L$,

$$\sum_{\ell=1\cdots W} \rho^\ell_{s,d,m} = \begin{cases} \mathfrak{a}_{\mathfrak{F}(\widetilde{\delta}_{s,d})} & \text{if } \mathfrak{e}_m \in p_{s,d}, \\ 0 & \text{otherwise.} \end{cases} \tag{18}$$

- In each scenario 's', each wavelength on a link can be used at most once at a given time instant. $\forall s = 0\cdots N$, $\forall m = 1\cdots L$, $\forall \ell = 1\cdots W$, $t = 1\cdots\mathfrak{T}$,

$$\sum_{d=1\cdots\widetilde{D}_s} \rho^\ell_{s,d,m} \times \widetilde{\theta}_{s,d,t} \leqslant 1 \tag{19}$$

- A path $p_{s,d}$ must use the same wavelength on any two consecutive links unless a regenerator is deployed at the node in common to the two links. $\forall s = 0\cdots N$, $\forall d = 1\cdots\widetilde{D}_s$, $\forall \ell = 1\cdots W$, $\forall \mathfrak{e}_m = (\mathfrak{u}_v, \mathfrak{u}_u) \in p_{s,d}$, $\forall \mathfrak{e}_n = (\mathfrak{u}_u, \mathfrak{u}_l) \in p_{s,d}$,

$$\rho^\ell_{s,d,m} - \rho^\ell_{s,d,n} \leqslant \mathfrak{d}_{s,d,u} \tag{20a}$$

$$\rho^\ell_{s,d,n} - \rho^\ell_{s,d,m} \leqslant \mathfrak{d}_{s,d,u} \tag{20b}$$

- The Q-factor at the destination node of a request must exceed the predefined threshold Q_{th}. Otherwise, a regenerator is deployed at an intermediate node along the path of the degraded request. $\forall s = 0\cdots N$, $\forall d = 1\cdots\widetilde{D}_s$, $\forall \ell = 1\cdots W$, $\forall \mathfrak{e}_m \in p_{s,d}$,

$$\mathfrak{Q}^\ell_{s,d} \times \rho^\ell_{s,d,m} + Q_{th} \times \sum_{\mathfrak{e}_n=(\mathfrak{u}_u,\mathfrak{u}_v)\in p_{s,d}\setminus \mathfrak{u}_u \neq \mathfrak{s}_{s,d}} \mathfrak{d}_{s,d,u} \geqslant Q_{th} \times \rho^\ell_{s,d,m} \tag{21}$$

- In each scenario 's', the number of regenerators $\psi_{s,u,t}$ in use at node $\mathfrak{u}_u$ and time instant τ_t is equal to the sum of:
  - the number of regenerators already deployed in the corresponding scenario 's' of the RRP sub-problem for the original requests that remained accepted,
  - and the number of regenerators added to serve as wavelength converters and/or to cope with the QoT degradation due to the non-flat spectral response of optical equipment.

These constraints allow the WARP sub-problem to reuse, when possible, the regenerators deployed in the RRP sub-problem. $\psi_{s,u,t}$ is computed as: $\forall s = 0\cdots N$, $\forall u = 1\cdots N$, $\forall t = 1\cdots\mathfrak{T}$,

$$\psi_{s,u,t} = \sum_{i=1\cdots\widehat{D}} \widehat{\theta}_{i,t} \times \widehat{\mathfrak{d}}_{s,i,u} \times \mathfrak{a}_i + \sum_{d=1\cdots\widetilde{D}_s} \widetilde{\theta}_{s,d,t} \times \mathfrak{d}_{s,d,u} \tag{22}$$

- The number of regenerators $\mathfrak{R}_u$ deployed at node $\mathfrak{u}_u$ is the maximum number of regenerators that are in use at any time for all the considered scenarios. $\forall s = 0\cdots N$, $\forall u = 1\cdots N$, $\forall t = 1\cdots\mathfrak{T}$,

$$\mathfrak{R}_u \geqslant \psi_{s,u,t} \tag{23}$$

- A node is considered as a regeneration node if it hosts at least a single regenerator. $\forall u = 1\cdots N$,

$$\phi_u \geqslant 10^{-3} \times \mathfrak{R}_u \tag{24}$$

- Finally, a regenerator pool failure at node $\mathfrak{u}_s$ is simulated by setting to zero the number of regenerators that can be deployed at this node in its corresponding scenario. $\forall s = 1\cdots N$, $\forall t = 1\cdots\mathfrak{T}$,

$$\psi_{s,s,t} = 0 \tag{25}$$

4) Objective: The objective of the WARP sub-problem remains the same as in the RRP sub-problem. We recall that this objective is expressed as:

$$\max \quad \gamma_1 \times \sum_{i=1\cdots D} \mathfrak{a}_i - \gamma_2 \times \sum_{u=1\cdots N} \phi_u - \gamma_3 \times \sum_{u=1\cdots N} \mathfrak{R}_u \tag{26}$$

IV. Numerical Results

In this paper, we aim to emphasize the cost benefit brought by the $M : N$ shared regenerator protection scheme. To the best of our knowledge, this is the first paper to deal with the optimal translucent network design taking into account both operational and backup regenerators. Thus, the only available reference scenario is the 1 : 1 regenerator protection scheme. For the sake of fairness, we consider an exact approach for the 1 : 1 regenerator protection scheme. This is achieved by recalling the work in [12] which computes the optimal number of regenerators and regeneration nodes without any consideration of network survivability. The 1 : 1 regenerator protection scheme can be derived from the latter approach by deploying two identical regenerator pools at each regeneration node; one pool of regenerators serving during normal operations and the other dedicated to backup operations.

In the sequel, we compare the results of the proposed model with the results of the reference scenario in terms of average acceptance ratio $\bar{a}$, average number of regeneration nodes $\bar{\phi}$, as well as average number of regenerators $\bar{\mathfrak{R}}$. For each request, we compute beforehand 5-shortest paths between its source and destination nodes. The parameters γ_1, γ_2, and γ_3 are set to 10^3, 1, and 10^{-3}, respectively. In other words, our main objective is to maximize the number of accepted requests, then we give higher priority to regenerator concentration over minimizing the number of regenerators. It should be noted that the number of regenerators additionally deployed in the WARP sub-problem rarely exceeds 2 regenerators. These additional regenerators are used to overcome the dependency of the signal quality on the assigned wavelength and to alleviate the wavelength continuity constraint. This demonstrates that decomposing the translucent network design problem into RRP and WARP sub-problems does not sacrifice the optimality of the final result.

A. Translucent NSF Network Design

In this section, we consider 10 sets of 200 SLDs where the activity period π is set to 0.4. For these traffic sets, we compute the optimal number of regenerators and the optimal distribution of regeneration nodes under 1 : 1 and $M : N$ regenerator protection schemes. It is worth noting that all the SLDs are accepted for all the considered sets of requests and for both protection schemes. Moreover, we should highlight that 9 nodes out of 14 (u_1, u_2, u_3, u_7, u_8, u_{11}, u_{12}, u_{13}, and u_{14}) are never selected as regeneration nodes in both protection schemes.

Under 1 : 1 regenerator protection scheme, the optimal number of regeneration nodes varies between 1 and 2 with an average value $\bar{\phi}$ equal to 1.6 regeneration nodes. The optimal number of regenerators varies between 52 and 66 with an average value $\bar{\mathfrak{R}}$ equal to 57.33 regenerators. Under $M : N$ shared regenerator protection scheme, the optimal number of regeneration nodes is always equal to 3 and the optimal number of regenerators varies between 40 and 50 with an average value $\bar{\mathfrak{R}}$ equal to 43.33 regenerators. This represents an average gain of 24.4% in terms of number of deployed regenerators.

Let us detail the solution of the translucent network design for a randomly selected set of 200 SLDs. Under 1 : 1 regenerator protection scheme, nodes u_4 and u_{10} are selected as the optimal regeneration nodes. Node u_4 contains two regenerator pools of 23 regenerators each, while node u_{10} contains two regenerator pools of 6 regenerators each. This corresponds to a total of 2 regeneration nodes and 58 regenerators. For the same set of SLDs, nodes u_4, u_5, and u_{10} are selected as the optimal regeneration nodes under $M : N$ shared regenerator protection scheme. The optimal number of regenerators at nodes u_4, u_5, and u_{10} is equal to 15, 15, and 14, respectively. This corresponds to a total of 3 regeneration nodes and 44 regenerators. During the normal operations of the network where all the regenerator pools are fully operational (Scenario '0'), 11 regenerators are used at node u_4, 12 regenerators are used at node u_5, and 6 regenerators are used at node u_{10}. When we assume that the regenerator pool at node u_4 has failed (Scenario '4'), 15 regenerators are needed at node u_5 and 14 regenerators are needed at node u_{10} in order to accommodate the 200 SLDs. Similarly, when we assume that the regenerator pool at node u_5 has failed (Scenario '5'), 15 regenerators are needed at node u_4 and 14 regenerators are needed at node u_{10}. Finally, when we assume that the regenerator pool at node u_{10} has failed (Scenario '10'), 14 regenerators are needed at node u_4 and 15 regenerators are needed at node u_5. To summarize, $N = 29$ operational regenerators are protected using $M = 44 - 29 = 15$ backup regenerators. This highlights the cost benefit brought by the $M : N$ shared regenerator protection scheme.

Furthermore, it should be noted that the number of SLDs that required regeneration varies between 40 and 41 requests according to the considered failure scenario. If we use a dedicated regenerator for each SLD requiring regeneration, the resulting routing solution would require 40 or 41 regenerators. However, thanks to the resource reutilization between time-disjoint SLDs, the number of regenerators used in these scenarios is only equal to 29 regenerators.

To conclude, we note that the optimal number of regeneration nodes for the NSF network under medium traffic loads, while ensuring network survivability, is equal to 3 nodes. Concentrating regenerators into 1 or 2 nodes exposes the network to a high risk of data loss in the eventual case of regenerator pool failure. Furthermore, we note that $M : N$ shared regenerator protection scheme evenly distributes the number of required regenerators over the regeneration nodes.

B. Impact of Traffic Load on Regenerator Distribution

In this section, we consider three different loads of permanent requests ($D \in \{100, 200, 300\}$). For each traffic load, we generate 10 sets of PLDs. Table II summarizes the results obtained for the different traffic loads considered in our evaluation. Figure 3 shows the *median* distribution of the deployed regenerators over the network nodes. It is obvious that the number of regenerators and regeneration nodes increase with the traffic load. For 100 PLDs, the $M : N$ and 1 : 1 protection schemes achieve the same results. However, the $M : N$ shared regenerator protection scheme achieves in average a reduction of 22% to 25% in the number of deployed regenerators compared to the 1 : 1 regenerator protection scheme for the sets of 200 and 300 PLDs.

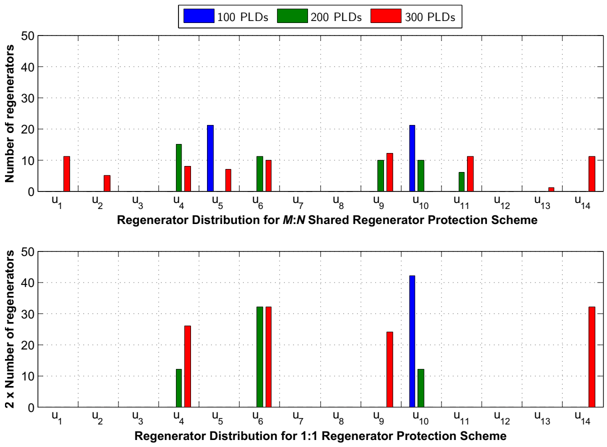

Fig. 3. Median regenerator distribution $\mathfrak{R}_u$ for various loads of PLDs.

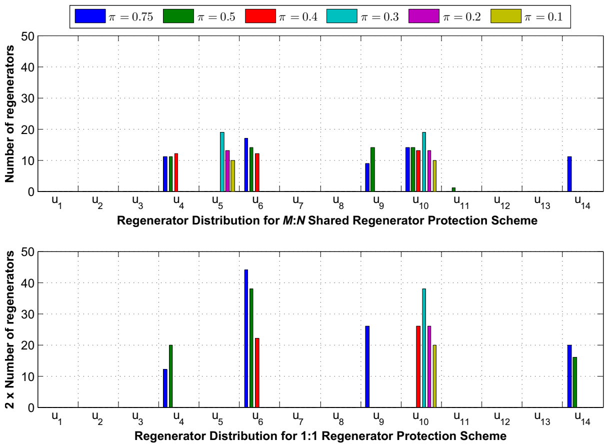

Fig. 4. Median regenerator distribution $\mathfrak{R}_u$ for various sets of 200 SLDs.

TABLE II
RESULTS FOR VARIOUS LOADS OF PERMANENT PLDS.

D	$M:N$ protection			$1:1$ protection		
	$\bar{a}$	$\bar{\phi}$	$\bar{\mathfrak{R}}$	$\bar{a}$	$\bar{\phi}$	$\bar{\mathfrak{R}}$
100	100%	2	42	100%	1	42
200	100%	4.33	48.67	100%	2.67	62.67
300	87.56%	9.33	87.33	88.33%	4	119.33

TABLE III
RESULTS FOR VARIOUS SETS OF 200 DYNAMIC SLDS.

π	$M:N$ protection			$1:1$ protection		
	$\bar{a}$	$\bar{\phi}$	$\bar{\mathfrak{R}}$	$\bar{a}$	$\bar{\phi}$	$\bar{\mathfrak{R}}$
0.75	100%	5.67	68	100%	3	96.67
0.5	100%	5.33	65.33	100%	3	85.33
0.4	100%	3	43.33	100%	1.6	57.33
0.3	100%	2	40.67	100%	1	40.67
0.2	100%	2	28.67	100%	1	28.67
0.1	100%	2	18.67	100%	1	18.67

C. Impact of Time-Correlation on Regenerator Distribution

In this section, we investigate the impact of the requests' time-correlation on the number of regenerators and regeneration nodes by considering dynamic requests with different activity periods ($\pi \in \{0.1, 0.2, 0.3, 0.4, 0.5, 0.75\}$). For each value of the time-correlation, we generate 10 sets of 200 SLDs. Table III summarizes the results obtained for the different sets of SLDs. Figure 4 shows the *median* distribution of the deployed regenerators over the network nodes. We notice that for small values of π ($\pi \in \{0.1, 0.2, 0.3\}$), the $M:N$ and $1:1$ regenerator protection schemes achieve the same results, and the nodes u_5 and u_{10} are the only regeneration nodes. For large values of π ($\pi \in \{0.4, 0.5, 0.75\}$), nodes u_4, u_6, u_9, and u_{10} host more than 80% of the deployed regenerators. Moreover, for the latter values, the reduction in the number of deployed regenerators varies between 23% and 30% when comparing the $M:N$ and $1:1$ regenerator protection schemes.

D. Translucent EBN Network Design

In this section, we consider the EBN backbone network and generate 10 different sets of 150 SLD requests with an activity period π of 0.4. In the case of $1:1$ protection scheme, all the SLDs are accepted, while in the $M:N$ protection scheme, the number of rejected SLDs varies between 10 and 19 with an average value of 14 rejected requests. This corresponds to an average acceptance ratio $\bar{a}$ of 90.66%. It is worth noting that nodes u_1, u_2, u_4, u_8, u_{13}, u_{18}, u_{20}, and u_{21} are never selected as regeneration nodes in both protection schemes.

In the case of $1:1$ protection scheme, the optimal number of regeneration nodes is always equal to 4 and the optimal number of regenerators varies between 96 and 132 with an average value $\bar{\mathfrak{R}}$ equal to 108 regenerators. In the case of $M:N$ protection scheme, the optimal number of regeneration nodes varies between 4 and 6 with an average value $\bar{\phi}$ equal to 5.6 regeneration nodes, while the optimal number of regenerators varies between 41 and 66 with an average value $\bar{\mathfrak{R}}$ equal to 51.4 regenerators. However, it is not fair to compute the average gain as the two protection schemes do not have the same rejection ratio.

V. CONCLUSION

Reducing the number of regenerators and regeneration nodes is highly motivated by the reduction in power consumption and maintenance cost. However, excessively concentrating the regenerators into a small number of nodes exposes the network to a high risk of data loss in the hazardous event of a regenerator pool failure. The same analysis is applicable if we investigate the failure of multi-channel all-optical regenerators instead of electrical regenerators pool. Indeed, a multi-channel all-optical regenerator can be used to simultaneously regenerate several wavelengths and the failure of such device will impact all the requests that are planned to be regenerated at this node.

Therefore, it is essential to keep in mind the network survivability concern while dimensioning the network. In this paper, we propose an exact approach based on a mathematical formulation that implements an $M:N$ shared regenerator protection scheme where N operational regenerators are protected using M backup regenerators. The proposed formulation compute the optimal number of regeneration nodes and seeks to evenly distribute the number of required regenerators over the regeneration nodes. In order to improve the scalability of our approach, we decompose the problem into the "Routing and

Regenerator Placement" (RRP) sub-problem and the "Wavelength Assignment and Regenerator Placement" (WARP) sub-problem. We showed that decomposing the original problem into two sub-problems does not sacrifice the optimality of the final result. Furthermore, in order to shorten the time needed to reach the optimal regenerator deployment solution, we tighten the formulation by adding constraints that will help discard equivalent solutions without omitting the optimal solution.

As a rule of thumb, we can conclude that when the deployed regenerators can be concentrated into a single regeneration node under the $1:1$ regenerator protection scheme, the $M:N$ shared regenerator protection scheme achieves comparable results to those obtained by the $1:1$ regenerator protection scheme. This is usually achieved by equally splitting the number of required regenerators over two distinct regeneration nodes. However, when the number of regenerator nodes increases, the $M:N$ shared regenerator protection scheme outperforms its counterparts by evenly distributing the number of required regenerators over several regeneration nodes. The gain obtained by the $M:N$ shared regenerator protection scheme may rapidly exceed 25% in terms of number of deployed regenerators.

References

[1] T. Schmidt, C. Malouin, R. Saunders, J. Hong, and R. Marcoccia, "Mitigating channel impairments in high capacity serial 40 G and 100 G DWDM transmission systems," in *Digest of the IEEE/LEOS Summer Topical Meetings*, 2008, pp. 141–142.

[2] A. Morea, N. Brogard, F. Leplingard, J.-C. Antona, T. Zami, B. Lavigne, and D. Bayart, "QoT function and a* routing: an optimized combination for connection search in translucent networks," *OSA JON*, vol. 7, no. 1, pp. 42–61, Jan. 2008.

[3] X. Yang and B. Ramamurthy, "Sparse regeneration in translucent wavelength-routed optical networks: architecture, network design and wavelength routing," *Springer PNC*, vol. 10, no. 1, pp. 39–50, Jul. 2005.

[4] G. Shen, W. Grover, T. Cheng, and S. Bose, "Sparse placement of electronic switching nodes for low-blocking in translucent optical networks," *OSA JON*, vol. 1, no. 12, pp. 424–441, Dec. 2002.

[5] Q. Rahman, Y. Aneja, S. Bandyopadhyay, and A. Jaekel, "Optimal regenerator placement in survivable translucent networks," in *Proc. of IEEE DRCN*, 2014.

[6] R. Ramlall, Q. Rahman, Y. Aneja, and S. Bandyopadhyay, "Optimal regenerator placement for path protection in impairment-aware WDM networks," in *Proc. of IEEE HPSR*, 2015.

[7] M. Youssef, S. Al Zahr, and M. Gagnaire, "Translucent network design from a CapEx/OpEx perspective," *Springer PNC*, vol. 22, no. 1, pp. 85–97, Aug. 2011.

[8] S. Pachnicke, T. Paschenda, and P. Krummrich, "Assessment of a constraint-based routing algorithm for translucent 10 Gbits/s DWDM networks considering fiber nonlinearities," *OSA JON*, vol. 7, no. 4, pp. 365–377, Apr. 2008.

[9] Z. Pan, B. Chatelain, D. Plant, F. Gagnon, C. Tremblay, and E. Bernier, "Tabu search optimization in translucent network regenerator allocation," in *Proc. of IEEE BROADNETS*, 2008, pp. 627–631.

[10] W. Zhang, J. Tang, K. Nygard, and C. Wang, "Repare: Regenerator placement and routing establishment in translucent networks," in *Proc. of IEEE GLOBECOM*, 2009, pp. 1–7.

[11] K. Manousakis, K. Christodoulopoulos, E. Kamitsas, I. Tomkos, and E. Varvarigos, "Offline impairment-aware routing and wavelength assignment algorithms in translucent WDM optical networks," *IEEE/OSA JLT*, vol. 27, no. 12, pp. 1866–1877, June 2009.

[12] E. A. Doumith, S. Al Zahr, and M. Gagnaire, "Mutual impact of traffic correlation and regenerator concentration in translucent WDM networks," in *Proc. of IEEE ICC*, 2011, pp. 1–6.

[13] S. Al Zahr, E. A. Doumith, and M. Gagnaire, "An exact approach for translucent WDM network design considering scheduled lightpath demands," in *Proc. of IEEE ICT*, 2011, pp. 450–457.

[14] M. Gagnaire, E. A. Doumith, and S. Al Zahr, "A novel exact approach for translucent WDM network design under traffic uncertainty," in *Proc. of IEEE ONDM*, 2011, pp. 1–6.

[15] F. Parmigiani, L. Provost, P. Petropoulos, D. J. Richardson, W. Freude, J. Leuthold, A. D. Ellis, and I. Tomkos, "Progress in multichannel all-optical regeneration based on fiber technology," *IEEE Journal of Selected Topics in Quantum Electronics*, vol. 18, no. 2, pp. 689–700, March 2012.

[16] S. Gringeri, V. Basch, B.and Shukla, R. Egorov, and T. J. Xia, "Flexible architectures for optical transport nodes and networks," *IEEE Communications Magazine*, vol. 48, no. 7, pp. 40–50, Jul. 2010.

[17] G. P. Agrawal, *Fiber optic communication systems*. Wiley-Interscience Publication, 1997.

[18] S. Al Zahr, "WDM translucent networks planning with guaranteed quality of transmission," https://pastel.archives-ouvertes.fr/pastel-00004014, École Nationale Supérieure des Télécommunications, Paris - France, 2007.